THE JOURNAL OF PHYSICAL CHEMISTRY B

Article

pubs.acs.org/JPCB

Bacteriochlorophyll Excited-State Quenching Pathways in Bacterial Reaction Centers with the Primary Donor Oxidized

Jie Pan,*[,†] Su Lin,[†,‡] and Neal W. Woodbury*[,†,‡]

[†]The Biodesign Institute at Arizona State University, Arizona State University, Tempe, Arizona 85287-5201, United States

[‡]Department of Chemistry and Biochemistry, Arizona State University, Tempe, Arizona 85287-1604, United States

Supporting Information

ABSTRACT: One striking feature of bacterial reaction centers is that while they show a high degree of structural symmetry, function is entirely asymmetric: excitation of the primary electron donor, P, a bacteriochlorophyll (BChl) dimer, results almost exclusively in electron transfer along one of the two symmetric electron transfer pathways. Here another functional asymmetry of the reaction center is explored; i.e., the two monomer BChl molecules (B_A and B_B) have distinct interactions with P in the oxidized state, P^+. Previous work has suggested that the excited states of both B_A and B_B were quenched via energy transfer to P^+ within a few hundred femtoseconds. Here, it is shown that various excitation wavelengths, corresponding to different initial B_A and B_B excited states, result in distinct reaction pathways, and which pathway dominates depends both on the initial excited state formed and on the electronic structure of P^+. In particular, it is possible to specifically excite the Q_X transition of B_B by using excitation at 495 nm directly into the carotenoid S_2 state which then undergoes energy transfer to B_B. This results in the formation of a new state on the picosecond time scale that is both much longer lived and spectrally different than what one would expect for a simple excited state. Combining results from additional measurements using nonselective 600 or 800 nm excitation of both B_A and B_B to the Q_X or Q_Y states, respectively, it is found that B_B* and B_A* are quenched by P^+ with different kinetics and mechanisms. B_A* formed using either Q_X or Q_Y excitation appears to decay rapidly (~200 fs) without a detectable intermediate. In contrast, B_B* formed via Q_X excitation predominantly generates the long-lived state referred to above via an electron transfer reaction from the Q_X excited state of B_B to P^+. This reaction is in competition with intramolecular relaxation of the Q_X state to the lowest singlet excited state. The Q_Y excited state of B_B appears to undergo the electron transfer reaction seen upon Q_X excitation only to a very limited extent and is largely quenched via energy transfer to P^+. Finally, the ability of P^+ to quench B_B* depends on the electronic structure of P^+. The asymmetric charge distribution between the two halves of P in the native reaction center is effectively reversed in the mutant HF(L168)/LH(L131), and in this case, the rate of quenching decreases significantly.

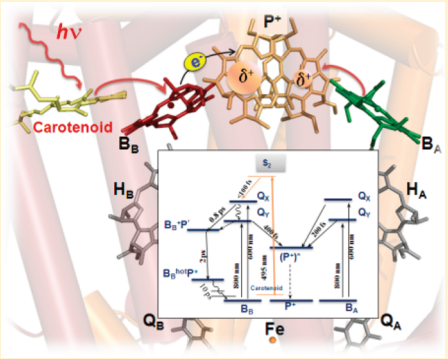

INTRODUCTION

Upon excitation of the photosynthetic apparatus with light, energy is normally transferred from excited antenna complexes to the photosynthetic reaction center where a multistep electron transfer process takes place.[1−6] The electron transfer cofactors in the *Rhodobacter (Rb.) sphaeroides* reaction center are arranged such that a bacteriochlorophyll (BChl) dimer that serves as the primary electron donor, P, is on the periplasmic side of the transmembrane complex and is immediately flanked by two monomer BChl molecules, B_A and B_B (Figure 1 and Figure S1, Supporting Information).[7] Progressing toward the cytoplasmic side of the complex, there are two bacteriopheophytin (BPhe) molecules (H_A and H_B) and two quinones (Q_A and Q_B). Near B_B there is a carotenoid (which has no symmetric counterpart).[8] In contrast to the apparent quasi-C-2 symmetry of these cofactors, the electron transfer initiated from the excited primary electron donor is almost exclusively along the A-branch cofactors (Figure S1, Supporting Information), resulting in a transmembrane charge-separated state, $P^+Q_A^-$.[9,10] This inherent functional asymmetry between the quasi-symmetric halves of the reaction center arises in part from environmentally induced energetic differences in the cofactors between the two sides.[11−15]

P^+ is re-reduced after light-induced electron transfer by a soluble cytochrome C in vivo.[16,17] The time constants for recovery of a neutral state P are more than 5 orders of magnitude slower than energy transfer from the excited antenna[18−20] or neighboring reaction center pigments.[21−26]

As long as the primary electron donor remains oxidized, the reaction center cannot process a second photon (the reaction center is "closed"). Under high light conditions, the steady-state population of closed reaction centers can become quite large. This is a potentially dangerous circumstance, particularly in organisms that exist in oxygenic environments; long-lived (bacterio)chlorophyll singlet excited states that are not rapidly quenched by normal electron transfer can convert from singlet to triplet and interact with oxygen to form singlet oxygen. The

Received: December 23, 2011
Published: January 9, 2012

ACS Publications © 2012 American Chemical Society

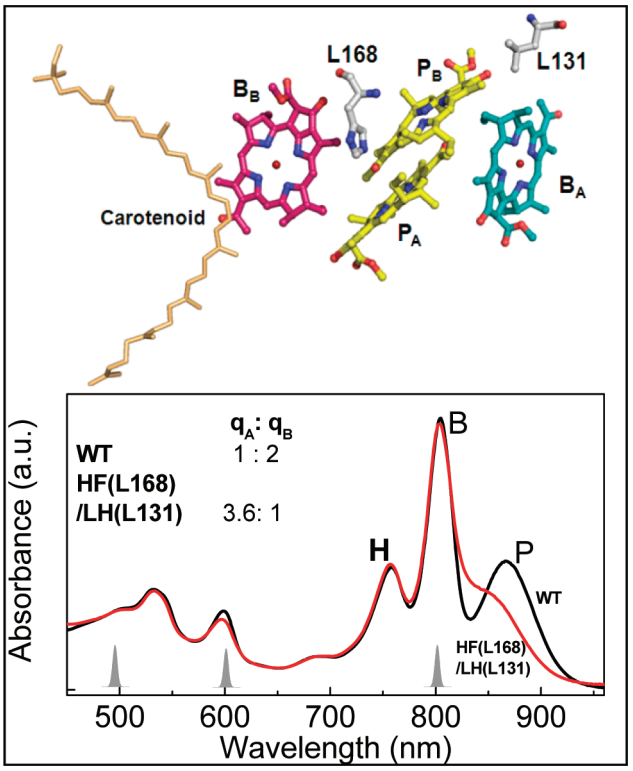

Figure 1. Upper panel: Structure of the bacteriochlorophyll (BChl) dimer, P, and the two quasi-symmetric monomer-BChl molecules that flank it to either side, B_A and B_B, in wild-type (WT) reaction centers from *Rb. sphaeroides* (PDB code: 2J8C). The bacteriochlorophyll phytol tails are not shown. Amino acid residues His L168 and Leu L131 and the 15,15′-*cis*-configuration carotenoid are shown as well. Color code: P, yellow; B_A, cyan; B_B, magenta; the carotenoid, orange. The view is along the approximate twofold symmetry axis of the protein from the periplasmic side of the complex. Lower panel: Absorption spectra of reaction center from the WT *Rb. sphaeroides* (black curve) and from the HF(L168)/LH(L131) mutant (red curve). The spectra of these two types of reaction center samples are normalized at the peak of the B-band at 802 nm. The Gaussian profiles shown under the spectra indicate excitation wavelengths (495, 600, and 800 nm) used in the transient absorption measurements. The relative spin density distributions, q_A:q_B, of P^+ between the two dimer bacteriochlorophylls, P_A and P_B, are shown for wild type and for the HF(L168)/LH(L131) mutant from ref 54.

singlet excited states themselves are also potentially reactive. Photosynthetic organisms have evolved a variety of mechanisms to rapidly quench unproductive excited states. The best studied of these is energy transfer to carotenoids.[27−30] In addition, the oxidized electron donor itself is often able to act as an excited-state quencher,[23,31−34] so that when the reaction center is closed, the system is not generating long-lived, reactive excited singlet states.

The mechanism of quenching in oxidized (closed) reaction centers is not well understood. In *Rb. sphaeroides,* excitation of whole photosynthetic membranes has shown that upon either photo-oxidation or chemical oxidation of the primary donor, P, the quenching time of the antenna excited states increases by only about a factor of 4 compared to open reaction centers (35−50 vs 200 ps, respectively),[19,35,36] still significantly shorter than the intrinsic excited-state lifetime of LH1 in the absence of energy transfer to the reaction centers (0.7 ns)[37] and of BChl molecules in solution (nanoseconds).[38] In addition to quenching antenna excited states, however, there is also the need to quench excited states in the reaction center itself under these conditions, as the reaction center cofactors will absorb light and form potentially destructive high-energy species. While the frequency of direct reaction center excitation is much lower than antenna excitation, unquenched local excitation in the reaction center is still quite a serious problem, as the reaction center is metabolically very expensive relative to antenna complexes.

In open *Rb. sphaeroides* reaction centers, BChl excited states, whether formed directly by light absorption or via energy transfer from BPhe,[25,39] are quenched by energy transfer to P, on the time scale of 100−200 fs.[23−26,40,41] The monomer BChl excited states persist for more than a nanosecond in a mutant where the absorbance band of P is missing.[32] However, in closed reaction centers (P^+), the excited BChl singlet states are quenched within a few hundred femtoseconds, as demonstrated by both transient absorbance[23,32,33] and up-conversion (ultrafast transient fluorescence) measurements.[34] Thus, P^+ plays a key role in removing unproductive local excited states and avoiding photodegradation of the reaction center.

It has been suggested that quenching of reaction center excited states by P^+ may involve energy transfer directly from B* to P^+.[42] It is also possible that B* transfers an electron to P^+, forming a state in which B is oxidized and P is neutral (B^+P). That charge-separated state would presumably return rapidly to the original state (BP^+) via back electron transfer, dissipating the energy as heat. Either mechanism should include an intermediate state, either an excited state of P^+ or a transient B^+P state, neither of which has been observed. One of the problems in trying to study this process is that neither excitation near 800 nm (the Q_Y band of the monomer BChls) nor 600 nm (the Q_X band of the monomer BChls) specifically excites one BChl or the other (a similar issue exists with overlapping absorbance bands of H_A and H_B, at least at physiological temperatures). As a result, excitation at these wavelengths results in multiple initial excited states, complicating the analysis. In particular, it becomes difficult to search for short-lived intermediates, as kinetic complexity may arise simply from the heterogeneous initial state.

In this work, the problem of multiple initial excited states is solved by indirect excitation specifically of B_B via the neighboring carotenoid. This is possible because the carotenoid has a unique absorbance at 495 nm and undergoes very fast and relatively efficient energy transfer to B_B, forming essentially pure B_B* on the 100 fs time scale.[43,44] In this way, one can cleanly investigate the formation of any transient intermediates in the quenching mechanism of B_B*. Combining these results with additional measurements using nonselective 600 and 800 nm excitation, different quenching dynamics from the excited states of each monomer BChl are resolved. Moreover, different reactions are found to take place from the Q_X and Q_Y states of B_B* in wild-type reaction centers containing an oxidized primary donor.

MATERIALS AND METHODS

Sample Preparation. Wild-type reaction centers from *Rb. sphaeroides* were expressed with a polyhistidine (poly-His) tag.[45] Construction of the mutant HF(L168)/LH(L131)) was performed on the poly-His wild-type background, following procedures described previously.[46,47] The codons for Leu L131 (CTG) and His L168 (CAT) were changed to His (CAT) and Phe (TTT), respectively. Reaction center purification was performed as described previously.[47] For spectroscopic

dx.doi.org/10.1021/jp212441b | *J. Phys. Chem. B* 2012, 116, 2014−2022

measurements, reaction centers were suspended in a buffer solution of 50 mM Tris-HCl (pH 8.0), 0.025% LDAO, 1 mM EDTA. All measurements were performed at room temperature.

Femtosecond Transient Absorption Spectroscopy. A pump−probe transient absorbance spectrophotometer was used to obtain time-resolved absorbance difference spectra. The general apparatus used has been described previously.[44] Briefly, pump pulses at 495 and 600 nm were generated in a home-built noncollinear optical parametric amplifier (NOPA). For 800 nm excitation, fundamental pulses from an amplified Ti:Sapphire laser (Spitfire, Spectra physics) were used directly. The broad-band probe pulses were generated by focusing a weak 800 nm beam into a 3 mm sapphire plate and sent to an optical compressor composed of a pair of prisms (CVI), before it was focused onto the sample. The polarization of the pump pulses was set to the magic angle (54.7°) with respect to that of the probe pulses. For near-IR measurements, data were collected over a 150 nm spectral range centered at 830 nm, with a spectral resolution of ∼1.2 nm. For visible region measurements, the spectral window was 500−760 nm with a spectral resolution of ∼2.4 nm. Reaction center samples were contained within a 2 mm path length cuvette, stirred with a small magnetic bar. Because the charge-separated state, $P^+Q_A^-$, lives for 100 ms before recombining, it was possible to photoaccumulate the primary electron donor, P, in the oxidized state, P^+, simply by stirring slowly enough so that the 1 kHz excitation beam created the charge-separated state much faster than it recombined. Following ref 34, 0.1 mM menadione was added, in order to maintain a high steady-state population of the P^+ state. Time-resolved spectra were corrected for spectral dispersion. Data analysis was performed using a global fitting program as in ref 44.

RESULTS

Spectrally Distinct Intermediate States in the Decay of B_B* in Oxidized Wild-Type Reaction Centers. Transient absorbance change spectra in the near-IR region (Q_Y transitions of BChl and BPhe) for wild-type reaction centers after excitation of the carotenoid at 495 nm are shown in Figure 2a. At a few hundred femtoseconds time delay, the major spectral features consist of a large absorption decrease centered near 800 nm and a broad absorbance increase below 780 nm. While the initially populated carotenoid S_2 state has a broad excited-state absorbance in this region,[48] energy transfer from the carotenoid S_2 state to B_B occurs in less than 100 fs;[44] therefore, by 200−300 fs, the transient absorbance spectra should reflect predominantly the spectral properties of B_B*. Note that there is no significant bleaching observed at this time in the ground-state Q_Y band of P at 865 nm (Figure 1 bottom), because P is maintained in a photo-oxidized state during the measurements.

The spectral evolution of the absorbance change in the 800 nm region involves more than simply the recovery of the B_B ground-state bleaching as B_B* decays. The decay of the broad positive band below 780 nm occurs in concert with an overall recovery of the 800 nm bleaching band. In addition to that, the long-wavelength side of the 800 nm absorbance decrease disappears more rapidly than the short-wavelength side. This initial spectral evolution takes several picoseconds. At the end of this time, a derivative-shaped feature has developed, with a zero-crossing point near 808 nm. The latter signal decays over the subsequent 10 ps. At long times (beyond ∼20 ps), a very small signal remains. It has the spectral characteristics of charge-separated states ($P^+H_A^-$ and $P^+Q_A^-$[3,25,26]) presumably arising from a small fraction of reaction centers that were not photo-oxidized.

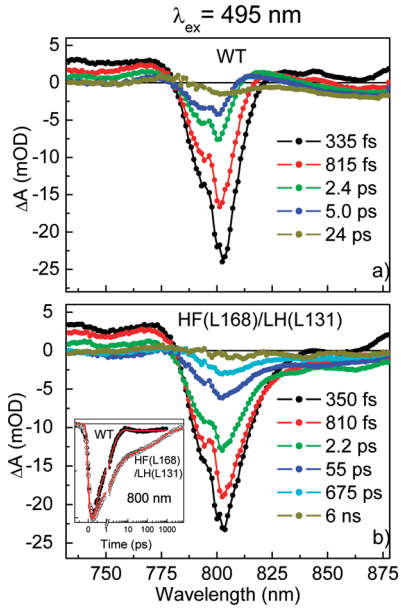

Figure 2. Time-resolved absorbance changes in the Q_Y spectral region recorded in (a) WT and (b) HF(L168)/LH(L131) mutant reaction centers after excitation of the carotenoid at 495 nm. Data points are shown as solid symbols with a smooth curve drawn through the points. The spectral resolution is ∼1.2 nm. Inset: Normalized kinetic traces at 800 nm from WT (filled circles, ●) and HF(L168)/LH(L131) mutant (opened circles, ○) reaction centers, after excitation at 495 nm. The solid lines represent the results of fitting. Note the time axis is linear until 1 ps and then logarithmic to 7 ns.

What is most striking about the spectral evolution described above is that parts of the bleaching in the 800 nm region take picoseconds to decay. This is in contrast to previous reports using fluorescence up-conversion and transient absorption approaches with 800 nm excitation (both B_A and B_B are excited) that the excited states of B decay predominantly on the few hundred femtosecond time scale in the presence of P^+.[23,32−34] In addition, the progressive profile changes of the spectra would be not expected for a simple excited-state decay of B_B*. The apparent kinetic and spectral discrepancy between the transient absorbance measurements presented here and previous measurements implies that either the 495 nm excitation wavelength used here leads to a different decay process or there are states generated from B_B* decay that were not reflected in previous measurements, or both.

Direct, Nonselective Excitation of the Monomer BChls at 600 and 800 nm. In order to explore the issues raised above, comparative measurements were performed on oxidized (P^+) wild-type reaction centers using 800 nm excitation. Excitation at 800 nm has been used previously for nonselective excitation of the Q_Y transitions of both B_A and B_B. In addition, since the excited-state energy from the carotenoid S_2 state is transferred predominantly to BChl via the Q_X transition,[49,50] direct excitation of the Q_X transition using 600 nm pulses was also performed on oxidized wild-type reaction centers. This should effectively mimic the indirect generation of B_B* via 495 nm excitation, though in a background of B_A excitation.

dx.doi.org/10.1021/jp212441b | J. Phys. Chem. B 2012, 116, 2014−2022

Kinetics at 800 nm using 495, 600, and 800 nm excitation are compared in Figure 3a. Traces from 600 and 800 nm excitation

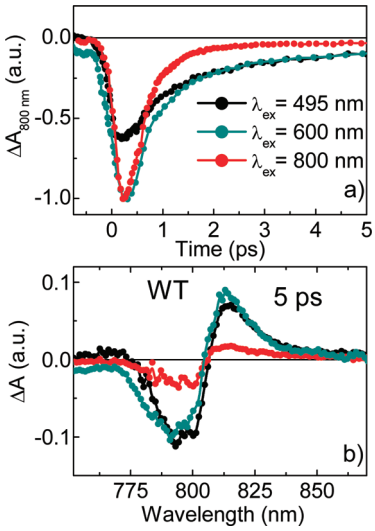

Figure 3. Comparison of kinetic traces at a probe wavelength of 800 nm (a) and transient absorption spectra in the Q_Y spectral region for WT reaction centers at 5 ps time delay (b), following excitation at 800 nm (red curve), 600 nm (dark cyan curve), and 495 nm (black curve). The amplitude of the 600 and 800 nm excitation kinetic traces in (a) are normalized, and the same factors were used to scale their spectra in (b). The normalization factors were chosen to show that the early-time decays using 600 and 800 nm excitation are very similar, while the long-time decays using 495 and 600 nm excitation are very similar. The contribution of signals from $P^+H_A^-$ and/or $P^+Q_A^-$ arising from residual open reaction centers (P in neutral state) is removed by subtracting the transient absorbance spectra recorded at 90 ps from that at 5 ps.

are normalized at their maxima, and the trace from 495 nm excitation was scaled such that its signal at 5 ps decay overlays that from the 600 nm excitation. Nearly half of the negative amplitude of the traces generated using 600 and 800 nm excitation recovers on the subpicosecond time scale, and the decay kinetics using these two excitation wavelengths are very similar. However, after this initial fast phase of decay, the kinetics of these two signals diverge, and the kinetics using 600 nm excitation are much slower than those using 800 nm excitation. After the initial 1.5 ps, the kinetics of the 600 nm excitation trace are essentially identical with those generated using 495 nm excitation. The time-resolved spectra at 5 ps are compared in Figure 3b for the three excitation conditions, using the same scaling factors as in Figure 3a. The derivative-shaped spectrum on a few picosecond time scale described above in the 495 nm excitation measurement is also observed using 600 and 800 nm excitation. However, this component (5 ps spectra in Figure 3b) represents a much larger fraction of the total signal when 495 or 600 nm excitation is used than it does when 800 nm excitation is used.

The fact that excitation at either 600 or 800 nm results in a fast phase that is largely missing when B_B is specifically excited via 495 nm excitation implies that much of the fast decay observed is due to B_A* decay, while the slower decay is predominantly due to B_B* decay. Apparently, the excited states of B_A and B_B interact differently with P^+. B_A* is rapidly quenched without a kinetically distinguishable intermediate, while B_B* generates a picosecond lifetime intermediate state. Further, this long-lived state is much more prevalent when B_B is excited via its Q_X transition than when it is excited via its Q_Y band.

To further characterize the quenching processes of B_A* and B_B*, transient absorption changes in the Q_Y region were recorded in an oxidized wild-type reaction center sample using 800 nm excitation. The black curves in Figure 4a and b show the kinetic traces at 750 and 807 nm, respectively. The former represents the decay of the broad positive band below 780 nm that presumably arises from excited-state absorption, and the latter reflects the ground-state bleaching recovery of both monomer-BChl molecules after 800 nm excitation. Two time constants of about 200 and 400 fs were obtained using a global analysis between 740 and 770 nm (Figure S2, Supporting Information), in reasonable agreement with previous work showing a single decay component of 250 fs using fluorescence up-conversion techniques.[34]

The long-lived state formed upon 800 nm excitation has a small amplitude, but it appears to be the same intermediate state generated using the other two excitation wavelengths, based on the spectral characteristics shown in Figure 3b. This state was explored in more detail in the Q_X region (Figure 4c). It was difficult to perform transient absorbance measurements in this spectral region using 495 nm excitation due to interference from a small amount of longer-lived carotenoid signals.[44] Using 800 nm excitation, the absorbance changes at early times, e.g., 100 fs, are dominant by a strong positive band peaking at 630 nm, indicative of a BChl excited state. A dip at 600 nm is also observed, as expected for ground-state bleaching of B*. The amplitude of the sharp absorbance increase at 630 nm decreases rapidly in the next 200 fs, accompanied by a change in spectral shape. After a few picoseconds, a new spectral feature develops with an absorbance maximum at 618 nm and an absorbance minimum at 585 nm (Figure 4c, magenta curve). This feature decays in roughly 10 ps, giving rise by 20 ps to a residual absorbance change that is presumably due to a small amount of $P^+H_A^-$ generated from the fraction of reaction centers that were not photo-oxidized.[3,13,51] The formation and decay dynamics of the picosecond spectral feature in the 600 nm region are essentially the same as that of the spectral feature observed near 800 nm (Figures 3b and 2a).

Decay of B_A* and B_B* in Oxidized HF(L168)/LH(L131) Mutant Reaction Centers. Transient absorption measurements of wild-type reaction centers using various excitation wavelengths have revealed distinct spectral and kinetic behaviors of B_A* and B_B*. ENDOR measurements have shown that the charge distribution in P^+ is asymmetric in wild-type reaction centers.[52,53] Asymmetry in the electronic structure of P^+ could give rise to different interactions with B_B* vs B_A*, resulting in some of the observed differences between the excited-state dynamics and quenching mechanisms between these two excited states as described above. To explore this possibility, measurements similar to those described for wild type were performed on the mutant HF(L168)/LH(L131), in which the asymmetric charge distribution in P^+ is altered, with little change in the P/P^+ redox potential.[54]

In wild-type reaction centers, the charge distribution over the two BChl molecules of P (P_A and P_B) in the state P^+ favors P_B by a q_B/q_A ratio of about 2:1.[52,53] In HF(L168)/LH(L131), however, the charge distribution is reversed, resulting in a 1:3.6 ratio favoring P_A.[54] Because this mutant involves both the removal of an H-bond between the His residue at L168 and the $C3^1$-acetylcarbonyl group of ring I and the introduction of an

dx.doi.org/10.1021/jp212441b | J. Phys. Chem. B 2012, 116, 2014−2022

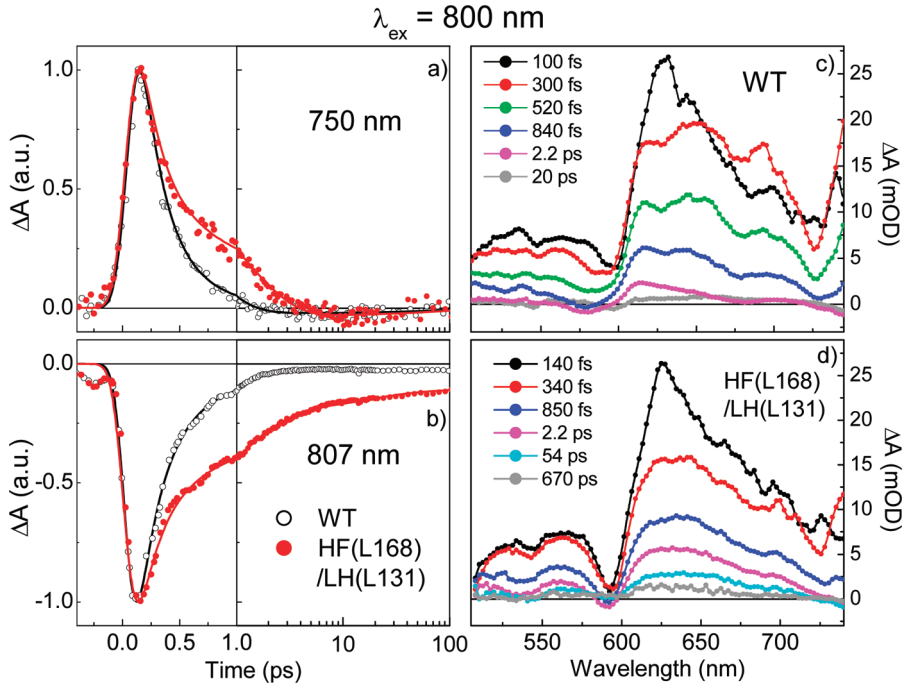

Figure 4. Panels (a) and (b): Normalized kinetic traces for WT (black open circles, ○) and HF(L168)/LH(L131) mutant reaction centers (red filled circles, ●). (a) Excited-state absorption at 750 nm. (b) Ground-state bleaching recovery at 807 nm. For these measurements, both monomer BChls, B_A and B_B, were excited at 800 nm. The solid lines represent the results from global multiple exponential fitting of the data. Note the time axis is linear until 1 ps and then logarithmic to 100 ps. Panels (c) and (d): Time-resolved absorbance change spectra in the Q_X spectral region recorded in (c) WT and (d) HF(L168)/LH(L131) mutant reaction centers after 800 nm excitation. Data points are shown as solid symbols with a smooth curve drawn through them. The spectral resolution is ~2.4 nm.

H-bond interaction with the 13^1-keto oxygen at ring V of the P_B (Figure 1, upper, and Figure S4, Supporting Information), the overall midpoint potential of P is largely unchanged (485 mV in the double mutant vs 505 mV in wild type).[54] The ground-state absorption spectrum of the double mutant differs from that of the wild-type reaction centers almost exclusively in the shape and position of the P-band (Figure 1, bottom).

495 nm Excitation. The absorbance change spectra in the Q_Y region for the double mutant as a function of time after excitation of carotenoid at 495 nm are shown in Figure 2b. There are both spectral and kinetic differences in the decay of B_B* compared to wild type (Figure 2a). First, the overall decay of the dominant absorbance changes in the 800 nm region is slower, a point that is more easily seen in the inset of Figure 2b, which compares the kinetics of the double mutant and wild type at 800 nm. The ground-state bleaching of B_B persists for hundreds of picoseconds in this mutant, raising the possibility that the excited state of B_B is long-lived. To investigate this further, fluorescence decay time measurements were performed using streak camera detection and 495 nm excitation. The streak camera is capable of measuring fluorescence emission spectra as a function of time with a 5 ps time resolution. A fluorescence signal from the HF(L168)/LH(L131) mutant was detected that persisted for hundreds of picoseconds (Figure S3, Supporting Information) in the double mutant. In contrast, essentially no B_B* fluorescence was observed from wild-type reaction centers, due to the short lifetime of this excited state in wild type compared to the time resolution of the instrument. The kinetic correspondence of the B_B ground-state bleaching decay and the measured fluorescence decay from B_B* in the double mutant implies that the observed long absorbance change recovery in the double mutant represents a slow decay of the excited state. The comparison of early-time transient absorption spectra, e.g., at 500 fs, of this mutant to that of wild type shows that the negative amplitude in the 800 nm region extends farther to the red in the mutant (Figure 5a). This is presumably due to the presence of the stimulated emission from the excited state of B_B, again consistent with the observation of fluorescence from the mutant (Figure S3, Supporting Information). Unlike wild type, there is no absorbance increase in the 815 nm region that develops on the picosecond time scale (Figure 2a, 5b and c). There is, however, a distinct very long-lived state (hundreds of picoseconds) that is formed in the HF(L168)/LH(L131) mutant involving BChl bleaching in the 800 nm region (Figure 2b), a bleaching at ~600 nm, and an additional bleaching at 540 nm (data not shown, but see next section, below). Moreover, the 600 and 540 nm signals have similar kinetics, suggesting that the very long-lived state is likely a small population of a charge-separated state involving B_B and H_B,[13,51,55] presumably in equilibrium with the B_B* that gives rise to the observed time-resolved fluorescence.

The key point of the mutant study using 495 nm excitation is that perturbation of the charge distribution in P^+ appears to slow down the quenching of B_B* by P^+, so that B_B* persists for hundreds of picoseconds. In addition, there is no clear evidence for any intermediate states of the kind observed in wild-type reaction centers with 495 nm excitation.

800 nm Excitation. A representative kinetic trace at 750 nm in the Q_Y region after 800 nm excitation on the HF(L168)/LH(L131) mutant reaction centers is shown in Figure 4a. The entire excited-state absorbance signal from 745 to 770 nm is shown in Figure S2 (Supporting Information). The excited-state decay in the mutant reaction centers, as measured by the

dx.doi.org/10.1021/jp212441b | J. Phys. Chem. B 2012, 116, 2014–2022

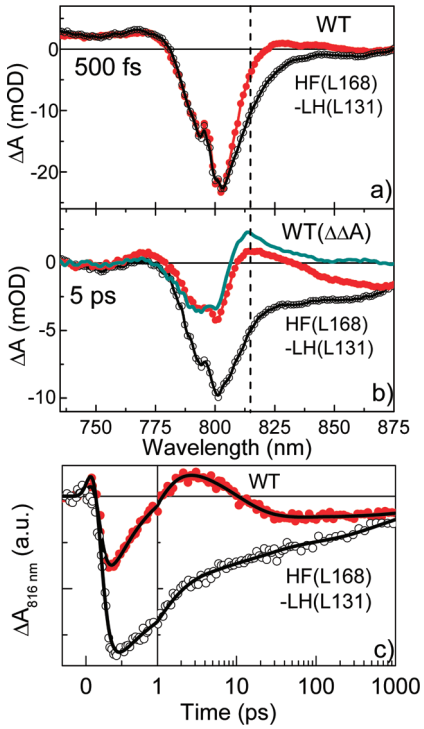

Figure 5. Transient absorption spectra of WT (red line) and HF(L168)/LH(L131) mutant (black line) reaction centers in the Q_Y spectral region recorded at different time delays following excitation at 495 nm: (a) 500 fs; (b) ~5 ps. The curves for HF(L168)/LH(L131) are uniformly scaled such that the bleaching maximum of the Q_Y transition near 800 nm at 500 fs is the same as that in wild type. The difference−difference spectrum between the WT transient absorption spectra recorded at 5 and 90 ps is calculated and shown as a cyan line. This was done to remove the contribution of signals due to charge-separated states arising from residual open reaction centers (P in neutral state). (c) Comparison of the kinetic traces recorded at a probe wavelength of 816 nm for WT (filled circles, ●) and HF(L168)/LH(L131) mutant (opened circles, ○) reaction center samples after excitation at 495 nm. The solid lines represent the results of global fitting analysis. Note the time axis is linear until 1 ps and then logarithmic to 1 ns.

decay of the 750 nm absorbance increase, differs in the mutant compared to wild type at times longer than 0.5 ps. In particular, there is a decay phase that is significantly longer than that observed in wild type. Similarly, measurements of the ground-state bleaching and stimulated emission of B* at 807 nm using 800 nm excitation (Figure 4b) again show that about half of the amplitude of this signal decreases much more slowly in the double mutant than that in wild type. Approximately 20% of the amplitude of the BChl ground-state bleaching remains after 100 ps. Comparing these results to those obtained using selective excitation of B_B* at 495 nm, it appears that the fast phase is present only when both B_A and B_B are excited at 800 nm. Thus the fast-decay phase (~200 fs) observed when 800 nm excitation is used in both the 750 and 807 nm kinetic traces (Figure 4a and b) presumably originates from B_A*. Given this, it appears that only the B_B* decay kinetics, but not the B_A* decay kinetics, are affected by modulating the charge distribution of P^+ in the mutant.

The absorbance change spectra in the Q_X region after 800 nm excitation for the mutant reaction centers are shown in Figure 4d. At 140 fs after excitation, the spectral profile is comparable to that of wild-type reaction centers (Figure 4c). In addition, the amplitude of the 630 nm band decays within 200 fs, as observed in wild type. However, the spectral profile and evolution of absorbance changes at later times in the mutant reaction centers, again, are different from that seen in wild type. The absorbance decrease centered near 600 nm due to ground-state bleaching of B* decays monotonically in the double mutant; neither the time-dependent band shifts nor a long-lived spectral feature similar to that of wild type after a few picoseconds (Figure 4c) were observed. Instead, small signals at long-time delays (hundreds of picoseconds) have spectral characteristics consistent with formation of a $B_B^+H_B^-$ charge-separated state,[13,51,55] which presumably explains the remaining BChl ground-state bleaching in the Q_Y region beyond 10 ps using 800 nm excitation in this mutant (Figure 4b, red curve).

DISCUSSION

Functional asymmetry of electron transfer is a well-known feature of purple bacterial reaction centers and is thought to originate mainly from the difference in reaction energetics of the two branches[11−13,15,56] and the asymmetry of the dielectric constant of the protein environments.[57] The observation that quenching of B_A and B_B excited states in closed reaction centers (containing P^+) is also asymmetric is therefore not too surprising. However, this asymmetry has not been as well studied as the directionality of electron transfer, in part because direct excitation of the monomer BChls is nonspecific, and therefore it is hard to assign function to one side or the other. Previous work has demonstrated quenching of excited monomer BChl by P on the 100−200 fs time scale, when P is either neutral or oxidized.[21−23,25,26,32−34,39] In general, this has been explained in terms of energy transfer, though electron transfer from B_A* to P (neutral) has been suggested from fitting of time-resolved spectral data.[58]

In this study, quenching of the excited states of B_A and B_B by P^+ has been explored in detail, taking advantage of the fact that excitation of the carotenoid indirectly results in selective formation of B_B*, and then comparing the spectral evolution under this condition with nonselective excitation in both the Q_X and Q_Y bands of the monomer BChls. The quenching pathway is found to depend on both which BChl is excited and whether or not it is excited directly into the lowest excited singlet state or a higher lying excited state. A qualitative representation of the reactions involved, based on the results described above, is given in Figure 6. This will serve as a basis for the discussion that follows.

The Decay Kinetics of B_A* and B_B* Quenched by P^+ Are Different. Past measurements of the excited-state quenching of B_A* and B_B* by P^+ have revealed multiple decay phases, particularly when transient absorption is used,[23,32,33] as opposed to fluorescence measurements.[34] Several different mechanisms have been proposed to explain this decay heterogeneity. For example, one explanation that has been advanced for the slower components of the decay is relaxation, either of P* or of ground-state B following B* to P energy transfer.[23]

Comparing selective (495 nm) and nonselective (600 or 800 nm) excitation of the monomer-BChls, it is clear that the resulting B_B* and B_A* are quenched by P^+ in ways that are both kinetically and probably mechanistically distinct. Excitation at 600 nm, which nonselectively excites B_A and B_B in the Q_X band, differs from excitation at 495 nm (indirectly producing B_B* via energy transfer from the carotenoid to the Q_X band of B_B) in that there is an additional fast phase. Because the additional fast

dx.doi.org/10.1021/jp212441b | J. Phys. Chem. B 2012, 116, 2014−2022

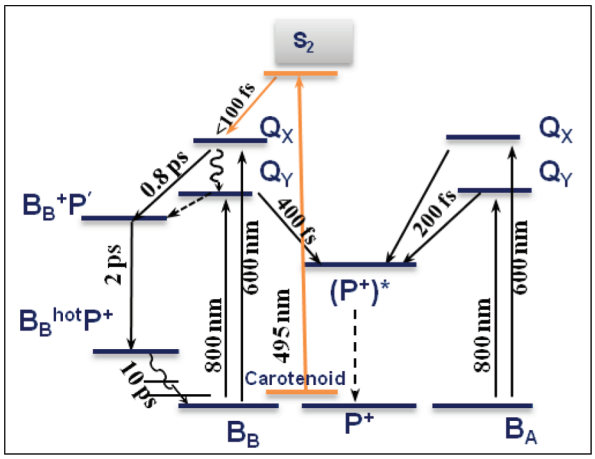

Figure 6. Qualitative reaction scheme illustrating the relevant states and relaxation pathways that may occur after formation of various excited states in wild-type reaction centers with P oxidized. Excitation at 495 nm (orange) generates the S_2 state of the carotenoid which selectively transfers excitation to the Q_X state of B_B within 100 fs.[44] Excitation at 600 nm generates the Q_X excited states of both B_A and B_B. Excitation at 800 nm results in formation of the lowest excited singlet states of both B_A and B_B (excited Q_Y transition). B_A excited in either the Q_X or Q_Y band transfers energy to P^+ within about 200 fs, while B_B excited in the Q_Y band transfers energy to P^+ in ~400 fs. The dashed line represents relaxation of the excited state(s) of P^+ (not resolved in this study). Direct or indirect excitation into the Q_X transition of B_B results in electron transfer to P^+, in competition with intramolecular relaxation to the Q_Y excited state. The 0.8 ps time constant for the B_B* to P^+ charge-separation reaction is estimated with an assumption of a 50% yield of charge separation. Because no spectral signature of a neutral ground-state P is observed in the transient absorption spectra, i.e., an absorbance increase at 865 nm, it is possible that neutral P is generated initially in an unrelaxed state, P′. Because charge recombination of the $B_B{}^+P'$ state apparently does not regenerate B_B ground state directly, a hot ground state of B_B may be formed immediately upon charge recombination and relax subsequently (see text for details). All reaction rates shown in the scheme were estimated based on the parameters obtained from global analysis of transient absorption data under various experimental conditions for wild-type reaction centers.

phase is only present when B_A is excited, it presumably represents quenching of B_A*. This fast phase appears to be essentially entirely the decay of ground-state bleaching (Figure 4a and b). However, the slower phase involves production of a signal that includes a positive absorbance change in the 815 nm region (Figure 3). Thus while B_A* formed using Q_X excitation seems to decay without a resolvable intermediate state, B_B* formed in this way appears to decay via a picosecond lifetime intermediate. Moreover, the ability of P^+ to quench B_B, with either Q_X or Q_Y excitation, depends on the electronic structure of P^+; when the electron density distribution between the two halves of P is reversed in the mutant HF(L168)/LH(L131), the rate of B_B* quenching is significantly slower, while no obvious effect is observed on the quenching kinetics of B_A*.

The Q_X and Q_Y States of B_B* Are Quenched by P^+ via Different Mechanisms. The fact that Q_X excitation (495 or 600 nm) of B_B results a decay path involving a picosecond lifetime intermediate, while B_A* decay appears to decay without a resolvable intermediate, suggests that a different mechanism must be involved in the P^+ quenching of B_B* than of B_A*. While one could imagine interactions between B_B and either the neighboring carotenoid or H_B, there is no spectral evidence for involvement of either cofactor, and teleologically, it would make much more sense for P^+ to quench excitation that cannot be processed in closed reaction centers. There are at least two types of mechanisms that could be used to explain B_B* quenching by P^+ in reaction centers: energy transfer in which the progression is $B_B{}^*P^+ \rightarrow B_BP^{+*} \rightarrow B_BP^+$ and electron transfer in which the progression is $B_B{}^*P^+ \rightarrow B_B{}^+P \rightarrow B_BP^+$. Both involve the formation of an intermediate state. While one cannot make an absolute assignment of mechanism to the decay mechanism of B_B* when excited into its Q_X band, there are a few clues that suggest that it decays via $B_B{}^+P$.

The first is simply that the decay of B_B* when excited in the Q_X band is clearly very different from that of either B_B or B_A when excited into the Q_Y band. Most of the quenching performed by P^+ is done in conjunction with antenna excited states. Given the distance between the antenna and P^+, this is presumably a dipole−dipole energy transfer. The antenna is in its lowest excited singlet state by the time that energy transfer to P^+ takes place. One might expect that the lowest excited singlet states of B_A and B_B would also be quenched predominantly via the same mechanism. Indeed, upon 800 nm excitation, the ground-state bleaching signals associated with both monomer BChls near 807 nm recover with about the same decay kinetics as the excited-state absorbance at 750 nm (Figure 4a and b). There are no obvious absorbance changes observed associated with P^{+*} (the intermediate state presumably formed upon energy transfer to P^+) in the spectral window between 500 to 1000 nm, though it is not clear that such an intermediate would have a long enough lifetime to be resolved.[59]

If it is true that Q_Y excitation decays via energy transfer, as suggested above, then the Q_X excited state of B_B presumably decays via a different pathway, forming a kinetically resolvable intermediate. The intermediate excited state of P^+ is unlikely to have a much longer lifetime simply because Q_X excitation of the monomer BChls is being used rather than Q_Y excitation. It seems more likely that B_B* is predominantly being quenched by a different mechanism when it is excited at 495 or 600 nm than it is exciting at 800 nm. The most likely alternative quenching mechanism for quenching of B_B* is charge separation, and the most likely electron acceptor is P^+ (electron transfer to H_B or the carotenoid would give rise to ground-state bleaching signals that are not observed). Electron transfer along alternate pathways initiated from high-lying excited states in the reaction center has been observed before,[51,55] and one might expect such an charge-separated intermediate to have a lifetime in the range of picoseconds.

A quenching mechanism involving electron transfer between B_B* and P^+ is also consistent with the observation that such a reaction is interrupted in a mutant that reverses the charge distribution in P^+ (HF(L168)/LH(L131)) (Figure 2b, 5b and c). One might expect that electron transfer would be strongly affected when the detailed structure and electron distribution in P^+ are changed.

Charge separation between the Q_X state of B_B* and P^+ would presumably give rise to a cation of B_B and a neutral P state. If, however, the state formed is $B_B{}^+P$, why is there no associated absorbance increase at 865 nm due to formation of the ground-state P? The only simple way to explain this is that the neutral P formed is not in the ground state. It remains in an unrelaxed state on this time scale. One possibility is that it may be in an electronic state that behaves more like two monomers than like a dimer. This is consistent with the absorbance increase

dx.doi.org/10.1021/jp212441b | J. Phys. Chem. B 2012, 116, 2014−2022

centered near 815 nm (Figure 2a and 5b). This B_B^+P' state recovers within 2 ps, but to a vibrationally hot state ($B_B^{hot}P^+$) which takes 10 ps to completely recover. Given this, an expanded scheme for the charge separation between B_B* and P^+ might be B_B*$P^+ \rightarrow B_B^+P' \rightarrow B_B^{hot}P^+ \rightarrow B_BP^+$ (Figure 6), where P′ is an unrelaxed form of neutral P. This would explain both the fact that the B_B bleaching persists long after B_B* has decayed and the fact that there is no absorbance increase associated with recovery of ground-state P at 865 nm.

It is not clear why the mechanism for quenching the upper excited states of B_B is different from that of B_A, either teleologically or structurally. Interaction between excited singlet states and radicals has been studied recently in a few molecular assemblies.[59,60] Several quenching mechanisms have been suggested, including parallel excited-state energy and hole-transfer pathways in oxidized porphyrin dyads, as well as competitive electron transfer and enhanced intersystem crossing processes in perylene dyads in different solvents. Given the well-defined molecular distances, orientations, and extensively characterized electronic structures of the relevant bacteriochlorin cofactors in the reaction center, it should be possible to explore this computationally. The current results do point out, as have previous reports,[51] that the upper excited states of reaction center BChl molecules live long enough to undergo chemistry, a fact that is relevant to photoprotection (see below). The functional asymmetry may have to do with B_B's somewhat special role as a triplet energy transfer intermediate between ^3P and the carotenoid.[44] Triplet energy transfer mechanisms typically involve what amounts to electron exchange which is effectively what appears to be happening from the Q_X excited state of B_B, though asynchronously.

Relevance to Photoprotection of Bacterial Reaction Centers. Photosynthetic systems must balance the need for creating high-energy states that are sufficiently long-lived to allow charge separation, while avoiding the destructive effects of these states on the apparatus itself to the extent possible. An additional balance is the need to create an apparatus that both efficiently utilizes low light levels and avoids damage from high light levels, when the apparatus effectively "backs up" and productive electron transfer can no longer remove excited states as fast as they are formed. One solution to the latter problem is clearly to create an initial electron donor with a dual function, acting both as an efficient reductant in the excited state and as an efficient quencher once it is oxidized. Further, this quencher must work with multiple excited states, those in both the antenna (long-range) and local excited states in the reaction center itself.

Of particular interest in this regard is that P^+ seems to quench the higher energy excited state of B_B (495 or 600 nm excitation) using a different mechanism, at least for the most part, than it does for quenching of neighboring molecules in the lowest excited singlet state. This must presumably decrease the time that B_B* remains in the higher excited state and thus decreases the likelihood of photodamage. What is perhaps most interesting is the fact that the environment of P and the neighboring cofactors has evolved to simultaneously optimize such a large number of different roles: optimizing forward electron transfer from P, minimizing recombination in the charge-separated states, and providing multiple mechanisms for rapidly quenching unwanted excitation when the reaction center is unable to process it. This points out the fact that while one often focuses on a single aspect of protein function, such as forward electron transfer in the case of the reaction center, and analyzes the system in terms of that alone, evolutionary forces may be involved in a much more complex balance of functional requirements.

■ ASSOCIATED CONTENT

Supporting Information

Additional materials and methods for streak camera time-resolved fluorescence measurements; arrangement of the *Rb. sphaeroides* reaction center cofactors, electron transfer scheme and associated time constants; 740−770 nm region transient absorption data of monomer BChl, B_A and B_B, in oxidized reaction centers of the wild-type and HF(L168)/LH(L131) mutant after 800 nm excitation; fluorescence emission trace recorded at probe wavelength of 800 ± 5 nm in the oxidized HF(L168)/LH(L131) mutant reaction centers by streak camera after excitation at 495 nm. This material is available free of charge via the Internet at http://pubs.acs.org.

■ AUTHOR INFORMATION

Corresponding Author

*E-mail Jie.Pan.1@asu.edu, tel. 480-965-0394, fax 480-727-0396 (J.P.); e-mail Nwoodbury@asu.edu, tel. 480-965-3294, fax 480-727-0396 (N.W.W.).

■ ACKNOWLEDGMENTS

This research was supported by NSF Grants MCB0642260 and MCB0640002 at ASU. The transient spectrometer used was funded by NSF Grant BIR9512970.

■ REFERENCES

(1) Parson, W. W.; Warshel, A. In *The purple phototrophic bacteria*; Hunter, C. N., Daldal, F., Thurnauer, M. C., Beatty, J. T., Eds.; Springer: Dordrecht, The Netherlands, 2009; pp 355−377.
(2) Woodbury, N. W.; Allen, J. P. In *Anoxygenic photosynthetic bacteria*; Blankenship, R. E., Madigan, M. T., Bauer, C. E., Eds.; Kluwer Academic Publishers: Dordrecht, The Netherlands, 1995; pp 527−557.
(3) Holzwarth, A. R.; Muller, M. G. *Biochemistry* **1996**, *35*, 11820−11831.
(4) Zinth, W.; Wachtveitl, J. *ChemPhysChem* **2005**, *6*, 871−880.
(5) Cogdell, R. J.; Gall, A.; Kohler, J. *Q. Rev. Biophys.* **2006**, *39*, 227−324.
(6) Pawlowicz, N. P.; Van Grondelle, R.; van Stokkum, I. H. M.; Breton, J.; Jones, M. R.; Groot, M. L. *Biophys. J.* **2008**, *95*, 1268−1284.
(7) Allen, J. P.; Feher, G.; Yeates, T. O.; Komiya, H.; Rees, D. C. *Proc. Natl. Acad. Sci. U.S.A.* **1987**, *84*, 5730−5734.
(8) Roszak, A. W.; McKendrick, K.; Gardiner, A. T.; Mitchell, I. A.; Isaacs, N. W.; Cogdell, R. J.; Hashimoto, H.; Frank, H. A. *Structure* **2004**, *12*, 765−773.
(9) Kirmaier, C.; Holten, D.; Parson, W. W. *Biochim. Biophys. Acta* **1985**, *810*, 33−48.
(10) Kirmaier, C.; Holten, D.; Parson, W. W. *Biochim. Biophys. Acta* **1985**, *810*, 49−61.
(11) Heller, B. A.; Holten, D.; Kirmaier, C. *Science* **1995**, *269*, 940−945.
(12) Wakeham, M. C.; Jones, M. R. *Biochem. Soc. Trans.* **2005**, *33*, 851−857.
(13) Chuang, J. I.; Boxer, S. G.; Holten, D.; Kirmaier, C. *Biochemistry* **2006**, *45*, 3845−3851.
(14) Williams, J. C.; Allen, J. P. In *The purple phototrophic bacteria*; Hunter, C. N., Daldal, F., Thurnauer, M. C., Beatty, J. T., Eds.; Springer: Dordrecht, The Netherlands, 2009; pp 337−353.
(15) LeBard, D. N.; Matyushov, D. V. *J. Phys. Chem. B* **2009**, *113*, 12424−12437.
(16) Moser, C. C.; Dutton, P. L. *Biochemistry* **1988**, *27*, 2450−2461.

(17) Tiede, D. M.; Vashishta, A. C.; Gunner, M. R. *Biochemistry* **1993**, *32*, 4515−4531.
(18) van Grondelle, R.; Dekker, J. P.; Gillbro, T.; Sundstrom, V. *Biochim. Biophys. Acta* **1994**, *1187*, 1−65.
(19) Timpmann, K.; Zhang, F. G.; Freiberg, A.; Sundstrom, V. *Biochim. Biophys. Acta* **1993**, *1183*, 185−193.
(20) Hu, X. C.; Ritz, T.; Damjanovic, A.; Autenrieth, F.; Schulten, K. *Q. Rev. Biophys.* **2002**, *35*, 1−62.
(21) Breton, J.; Martin, J. L.; Migus, A.; Antonetti, A.; Orszag, A. *Proc. Natl. Acad. Sci. U.S.A.* **1986**, *83*, 5121−5125.
(22) Breton, J.; Martin, J.-L.; Migus, A.; Antonetti, A.; Orszag, A. In *Ultrafast phenomena v*; Fleming, G. R., Siegman, A. E., Eds.; Springer-Verlag: New York, 1986; pp 393−397.
(23) Jia, Y. W.; Jonas, D. M.; Joo, T. H.; Nagasawa, Y.; Lang, M. J.; Fleming, G. R. *J. Phys. Chem.* **1995**, *99*, 6263−6266.
(24) Stanley, R. J.; King, B.; Boxer, S. G. *J. Phys. Chem.* **1996**, *100*, 12052−12059.
(25) Lin, S.; Taguchi, A. K. W.; Woodbury, N. W. *J. Phys. Chem.* **1996**, *100*, 17067−17078.
(26) Vos, M. H.; Breton, J.; Martin, J. L. *J. Phys. Chem. B* **1997**, *101*, 9820−9832.
(27) Frank, H. A.; Cogdell, R. J. In *Carotenoids in photosynthesis*; Young, A. J., Britton, G., Eds.; Chapman & Hall: London, U.K., 1993; pp 252−326.
(28) Ma, Y. Z.; Holt, N. E.; Li, X. P.; Niyogi, K. K.; Fleming, G. R. *Proc. Natl. Acad. Sci. U.S.A.* **2003**, *100*, 4377−4382.
(29) Frank, H. A.; Bautista, J. A.; Josue, J. S.; Young, A. J. *Biochemistry* **2000**, *39*, 2831−2837.
(30) Bode, S.; Quentmeier, C. C.; Liao, P. N.; Hafi, N.; Barros, T.; Wilk, L.; Bittner, F.; Walla, P. J. *Proc. Natl. Acad. Sci. U.S.A.* **2009**, *106*, 12311−12316.
(31) Slooten, L. *Biochim. Biophys. Acta* **1972**, *256*, 452−&.
(32) Jackson, J. A.; Lin, S.; Taguchi, A. K. W.; Williams, J. C.; Allen, J. P.; Woodbury, N. W. *J. Phys. Chem. B* **1997**, *101*, 5747−5754.
(33) Vulto, S. I. E.; Streltsov, A. M.; Shkuropatov, A. Y.; Shuvalov, V. A.; Aartsma, T. J. *J. Phys. Chem. B* **1997**, *101*, 7249−7255.
(34) King, B. A.; McAnaney, T. B.; de Winter, A.; Boxer, S. G. *Chem. Phys.* **2003**, *294*, 359−369.
(35) Sundstrom, V.; Vangrondelle, R.; Bergstrom, H.; Akesson, E.; Gillbro, T. *Biochim. Biophys. Acta* **1986**, *851*, 431−446.
(36) van Grondelle, R.; Bergström, H.; Sundström, V.; Gillbro, T. *Biochim. Biophys. Acta* **1987**, *894*, 313−326.
(37) Monshouwer, R.; Baltuska, A.; van Mourik, F.; van Grondelle, R. *J. Phys. Chem. A* **1998**, *102*, 4360−4371.
(38) Musewald, C.; Hartwich, G.; Pollinger-Dammer, F.; Lossau, H.; Scheer, H.; Michel-Beyerle, M. E. *J. Phys. Chem. B* **1998**, *102*, 8336−8342.
(39) King, B. A.; McAnaney, T. B.; deWinter, A.; Boxer, S. G. *J. Phys. Chem. B* **2000**, *104*, 8895−8902.
(40) Breton, J.; Martin, J. L.; Fleming, G. R.; Lambry, J. C. *Biochemistry* **1988**, *27*, 8276−8284.
(41) Haran, G.; Wynne, K.; Moser, C. C.; Dutton, P. L.; Hochstrasser, R. M. *J. Phys. Chem.* **1996**, *100*, 5562−5569.
(42) Jordanides, X. J.; Scholes, G. D.; Shapley, W. A.; Reimers, J. R.; Fleming, G. R. *J. Phys. Chem. B* **2004**, *108*, 1753−1765.
(43) Lin, S.; Katilius, E.; Ilagan, R. P.; Gibson, G. N.; Frank, H. A.; Woodbury, N. W. *J. Phys. Chem. B* **2006**, *110*, 15556−15563.
(44) Pan, J.; Lin, S.; Allen, J. P.; Williams, J. C.; Frank, H. A.; Woodbury, N. W. *J. Phys. Chem. B* **2011**, *115*, 7058−7068.
(45) Goldsmith, J. O.; Boxer, S. G. *Biochim. Biophys. Acta* **1996**, *1276*, 171−175.
(46) Williams, J. C.; Alden, R. G.; Murchison, H. A.; Peloquin, J. M.; Woodbury, N. W.; Allen, J. P. *Biochemistry* **1992**, *31*, 11029−11037.
(47) Katilius, E.; Babendure, J. L.; Lin, S.; Woodbury, N. W. *Photosynth. Res.* **2004**, *81*, 165−180.
(48) Cong, H.; Niedzwiedzki, D. M.; Gibson, G. N.; LaFountain, A. M.; Kelsh, R. M.; Gardiner, A. T.; Cogdell, R. J.; Frank, H. A. *J. Phys. Chem. B* **2008**, *112*, 10689−10703.
(49) Ricci, M.; Bradforth, S. E.; Jimenez, R.; Fleming, G. R. *Chem. Phys. Lett.* **1996**, *259*, 381−390.
(50) Krueger, B. P.; Scholes, G. D.; Fleming, G. R. *J. Phys. Chem. B* **1998**, *102*, 5378−5386.
(51) Lin, S.; Katilius, E.; Haffa, A. L. M.; Taguchi, A. K. W.; Woodbury, N. W. *Biochemistry* **2001**, *40*, 13767−13773.
(52) Lubitz, W.; Lendzian, F.; Bittl, R. *Acc. Chem. Res.* **2002**, *35*, 313−320.
(53) Daviso, E.; Prakash, S.; Alia, A.; Gast, P.; Neugebauer, J.; Jeschke, G.; Matysik, J. *Proc. Natl. Acad. Sci. U.S.A.* **2009**, *106*, 22281−22286.
(54) Rautter, J.; Lendzian, F.; Schulz, C.; Fetsch, A.; Kuhn, M.; Lin, X.; Williams, J. C.; Allen, J. P.; Lubitz, W. *Biochemistry* **1995**, *34*, 8130−8143.
(55) Haffa, A. L. M.; Lin, S.; Williams, J. C.; Taguchi, A. K. W.; Allen, J. P.; Woodbury, N. W. *J. Phys. Chem. B* **2003**, *107*, 12503−12510.
(56) Williams, J. C.; Allen, J. P. In *Advances in photosynthesis and respiration*; Hunter, C. N., Daldal, F., Thurnauer, M. C., Beatty, J. T., Eds.; Springer: New York, 2009; pp 337−353.
(57) Steffen, M. A.; Lao, K. Q.; Boxer, S. G. *Science* **1994**, *264*, 810−816.
(58) van Brederode, M. E.; van Mourik, F.; van Stokkum, I. H. M.; Jones, M. R.; van Grondelle, R. *Proc. Natl. Acad. Sci. U.S.A.* **1999**, *96*, 2054−2059.
(59) Song, H. E.; Kirmaier, C.; Diers, J. R.; Lindsey, J. S.; Bocian, D. F.; Holten, D. *J. Phys. Chem. B* **2009**, *113*, 54−63.
(60) Colvin, M. T.; Giacobbe, E. M.; Cohen, B.; Miura, T.; Scott, A. M.; Wasielewski, M. R. *J. Phys. Chem. A* **2010**, *114*, 1741−1748.